Journal of the Serbian Chemical Society
JSCS-info@shd.org.rs • www.shd.org.rs/JSCS
J. Serb. Chem. Soc. 91 (10) 1025–1041 (2026)
JSCS–5542
Original scientific paper
Published 18 November, 2026

A detailed thermodynamic analysis of a diesel engine at different compression ratios

HAKAN BAYRAKTAR[1] and İSMET SEZER[2]*

[1]*Karadeniz Technical University, Department of Mechanical Engineering, Faculty of Engineering, Trabzon, Türkiye and* [2]*Gümüşhane University, Department of Mechanical Engineering, Faculty of Engineering and Natural Sciences, Gümüşhane, Türkiye*

(Received 31 March, revised 25 May, accepted 6 October 2026)

Abstract: This study experimentally investigates the effects of compression ratio (*CR*) on the combustion, energy and exergy characteristics of a diesel engine. A four-stroke, naturally aspirated, water-cooled, direct-injection, single-cylinder diesel engine with variable *CR* capability was employed. Experiments were conducted at a constant speed of 1500 rpm under various loads, with *CR*s set to 15:1, 16:1 and 17:1. The software in the experimental setup calculated the arithmetic mean of ten cycles to minimize the effects of cycle-to-cycle variations and enhance the accuracy of the results. A detailed thermodynamic analysis was carried out to examine the combustion, energy and exergy characteristics of the tested *CR*s using data obtained from the experiments. The results demonstrated that *CR* has a significant influence on combustion, energy, and exergy characteristics. Combustion parameters such as mass burned fraction, heat release rate, cylinder pressure and gas temperature increased with rising *CR*. Similarly, performance indicators including efficiency, fuel consumption and the overall energy and exergy performance of the engine also tended to improve as *CR* increased. Among the tested *CR*s, a *CR* of 16 provided the most favorable exergetic outcomes. Specifically, exergy efficiency, exergy performance coefficient and sustainability index improved by 9.9–22.1, 45.3–110.9 and 0.6–6.9 %, respectively, depending on engine load for a *CR* of 16.

Keywords: combustion; exergy analysis; irreversibility; sustainability.

INTRODUCTION

Diesel engines are extensively employed in heavy duty applications such as transportation, construction and agriculture due to their low fuel consumption, high torque output and overall efficiency.[1] Single-cylinder diesel engines are frequently preferred as power sources in the agricultural sector, where they are commonly used to operate farming machinery such as water pumps, generators and tillers, as

* Corresponding author. E-mail: isezer@gumushane.edu.tr
https://doi.org/10.2298/JSC260331060B

Available online at https://www.shd.org.rs/JSCS/
(CC) 2026 Serbian Chemical Society.

well as in fishing activities.[2] However, the continuous rise in oil prices and the growing problem of environmental pollution have made it necessary to strengthen legal regulations and conduct technical studies aimed at improving the efficiency and environmental sustainability of internal combustion engines (ICEs).[3,4] Hence, intensive efforts have been directed toward utilizing renewable alternative fuels, improving the properties of fossil fuels, and developing ICEs in line with current technological advancements.[5,6] Improving fuel properties has made research on enhancing and optimizing engine design features increasingly important.[7,8] The compression ratio (*CR*) is one of the fundamental design parameters of ICEs and has a significant impact on combustion, performance and emission characteristics. Therefore, *CR* must be determined appropriately in accordance with the engine's structure and type, its charging system and the fuel characteristics.[9–11] Conversely, research on engines is conducted through theoretical and/or experimental approaches. While experimental studies provide more realistic results, they are often time-consuming and costly. Advances in computer and software technologies have increased the reliability of theoretical studies, making it possible to achieve desired outcomes with fewer experimental studies.[12,13] Theoretical and experimental studies on engines are primarily grounded in the principles of thermodynamics and fluid mechanics. Thermodynamics-based investigations often employ energy analysis derived from the first law of thermodynamics. However, it has been emphasized that exergy analysis, which supplements first-law approaches with those of the second law of thermodynamics, can yield more accurate results. Moreover, exergy analysis enables the identification of losses caused by system irreversibilities and supports efficiency improvements through studies aimed at reducing these losses.[14–16] For all these reasons, a detailed thermodynamic analysis was conducted in this study to investigate the effects of *CR* on the combustion, performance, energy and exergy characteristics of a diesel engine.

EXPERIMENTAL

The experimental setup comprises three primary components: the engine, the dynamometer and the measurement and control panel. An image of the test system is provided in Fig. 1. As illustrated, an electric dynamometer was incorporated into the system to impose a load on the engine, with the load being regulated through a dedicated switch.

The system is equipped with air, fuel and coolant tanks, along with measurement devices for air, fuel and coolant flow rates, torque, rotational speed, cylinder gas and fuel pressures and temperatures at various points. A data acquisition unit is integrated to transfer the recorded measurements to a computer. The performance parameters are subsequently calculated from the collected data using Enginesoft software, which operates on the Labview platform. The engine employed in the system is a four-stroke, naturally aspirated, water-cooled, direct-injection diesel engine, with its technical specifications presented in Table I. The *CR* of the engine can be adjusted through a mechanism located on the cylinder block. Experiments were carried out at a constant speed of 1500 rpm under varying load conditions ranging from 0 to 100 %. Measurements were recorded once the engine reached a steady–state operating regime, and the collected

(CC) 2026 Serbian Chemical Society.

data were utilized for a comprehensive thermodynamic analysis covering the combustion, performance, energy and exergy characteristics.[17]

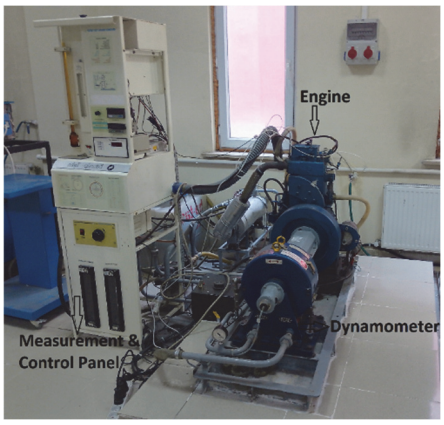

Fig. 1. Image of the experimental setup.

TABLE I. The specifications of the test engine[17]

Brand and model	Kirloskar TV1
Number of cylinders	1
Bore×Stroke	87.5 mm×110 mm
Cylinder volume	661 cm^3
Compression ratio	Variable
Engine power	3.5 kW @ 1500 rpm

The combustion, performance, energy, and exergy characteristics were identified and thoroughly analyzed using the equations provided below within the framework of thermodynamic evaluation. Various engine performance parameters, including power, efficiency, specific fuel consumption and the air excess coefficient, were determined accordingly. The indicated (in-cylinder) power (*IP*), brake power (*BP*) and friction (lost) power (*FP*) were calculated as follows:[18,19]

$$IP = \frac{WNZ}{60 \times CC \times 1000} \tag{1}$$

$$BP = \frac{2\pi N\tau}{60 \times 1000} \tag{2}$$

$$FP = IP - BP \tag{3}$$

The indicated specific fuel consumption (*ISFC*) and brake specific fuel consumption (*BSFC*) were calculated as follows:[18,19]

$$ISFC = \frac{\dot{m}_f}{IP} \tag{4}$$

$$BSFC = \frac{\dot{m}_f}{BP} \tag{5}$$

(CC) 2026 Serbian Chemical Society.

The indicated thermal efficiency (*ITE* or η_i), mechanical efficiency (*ME* or η_m) and brake thermal efficiency (*BTE* or η_e) were calculated as follows:[18,19]

$$ITE = \eta_i = \frac{3600IP}{\dot{m}_f LHV_f} \tag{6}$$

$$BTE = \eta_e = \frac{3600BP}{\dot{m}_f LHV_f} \tag{7}$$

In the energy analysis, the fuel energy (E_f), energy converted into work (E_W), energy lost with heat transfer (E_{cw}), energy lost with exhaust (E_{exh}) and other energy losses (E_{other}) were determined as follows:[19–21]

$$E_f = \dot{m}_f LHV_f \tag{8}$$

$$E_w = 3600BP \tag{9}$$

$$E_{cw} = \dot{m}_{cw} c_{p,cw} (T_2 - T_1) \tag{10}$$

$$E_{exh} = \left(\dot{m}_f + \dot{m}_h\right) c_{p,exh} (T_3 - T_0) \tag{11}$$

$$E_{other} = E_f - \left(E_w + E_{cw} + E_{exh}\right) \tag{12}$$

In the exergy analysis, the fuel exergy ($E_{\chi f}$), exergy converted into work ($E_{\chi w}$), exergy lost with heat transfer ($E_{\chi cw}$), exergy lost with exhaust ($E_{\chi exh}$) and exergy destruction ($E_{\chi dest}$) were determined as follows:[19–21]

$$E_{\chi_f} = \dot{m}_f \left[1.0401 + 0.1728\frac{h}{c} + 0.2169\frac{s}{c}\left(1 - 2.0628\frac{h}{c}\right)\right] \tag{13}$$

$$E_{\chi_w} = E_w \tag{14}$$

$$E_{\chi_{cw}} = E_{cw} + \left[\dot{m}_{cw} c_{p,w} T_2 \ln\left(\frac{T_1}{T_2}\right)\right] \tag{15}$$

$$E_{\chi_{exh}} = E_{exh} + \left[\left(\dot{m}_f + \dot{m}_h\right) c_{p,exh} T_0 \ln\left(\frac{T_0}{T_3}\right)\right] \tag{16}$$

$$E_{\chi_{dest}} = E_{\chi_f} - \left(E_{\chi_w} + E_{\chi_{cw}} + E_{\chi_{exh}}\right) \tag{17}$$

The exergy efficiency (η_{ex}), exergy performance coefficient (*EPC*) and sustainability index (*SI*) were also calculated as follows:[20–22]

$$\eta_{ex} = \frac{E_{\chi_w}}{E_{\chi_f}} \tag{18}$$

$$EPC = \frac{E_{\chi_w}}{E_{\chi_{dest}}} \tag{19}$$

$$SI = \frac{1}{1 - \eta_{ex}} \tag{20}$$

(CC) 2026 Serbian Chemical Society.

Uncertainties inevitably arise during experimental measurements due to the sensitivity of instruments, possible measurement errors and environmental conditions. Hence, uncertainty analysis is essential to demonstrate the accuracy of experimental results. In this study, the uncertainty analysis was carried out using the method described below. Any result parameter R is expressed as a function of the independent variables $x_1, x_2,\ldots,x_n$ as follows:[22]

$$R = R(x_1, x_2, \ldots, x_n) \tag{21}$$

Accordingly, the uncertainty U_R associated with any result parameter is determined as follows:

$$U_R = \sqrt{U_{R,1}^2 + U_{R,2}^2 + \ldots + U_{R,n}^2} = \sqrt{\sum_{i=1}^{n} U_{R,i}^2} \tag{22}$$

This approach, also referred to as the partial uncertainty method, determines the uncertainty $U_{R,i}$ arising from any independent variable x_i as follows:[22]

$$U_{R,i} = \left|\frac{\partial R}{\partial x_i}\right| U_i \qquad (1 \le i \le n) \tag{23}$$

The scale, sensitivity, and uncertainty values of the measurement devices, along with the uncertainty values of the main parameters calculated using this method, are shown in Table II.

TABLE II. Uncertainty values of devices and parameters

Measured parameter	Device	Scale	Sensitivity	Uncertainty, %
Engine load	Strain gauge	0–50 kg	±0.1 kg	±0.5
Engine speed	Magnetic sensor	0–10000 rpm	±10 rpm	±1
Pressure	Piezo sensor	0–5000 psi	±0.1 psi	±1
Crank angle	Magnetic sensor	–	±1 °CA	±0.2
Air flow rate	Pressure transducer	200 mm	1 mm	±1
Fuel flow rate	Pressure transducer	500 mmWC	1 mm	±1
Exhaust gas temperature	K-type thermocouple	0–1200 °C	±1 °C	±0.2
Brake torque	–	–	–	±0.5
Brake power	–	–	–	±1
Air excess coefficient	–	–	–	±1
Specific fuel consumption	–	–	–	±1.1
Brake thermal efficiency	–	–	–	±1.2

RESULTS AND DISCUSSION

Fig. 2a presents the variation in mass burned fraction (*MBF*) with crank angle at full load for different *CR*s. For all *CR*s, MBF increases rapidly with increasing crank angle, as shown in the figure. However, MBF begins to rise earlier at higher *CR*s. This behavior is attributed to the shortening of the ignition delay period, which leads to earlier and faster combustion since the in–cylinder gas pressure and temperature reach higher values as the *CR* increases. Fig. 2b illustrates the variation in heat release rate (*HRR*) with crank angle at full load for different *CR*s. Similar to *MBF*, the *HRR* rises earlier with increasing *CR* and it begins to decline sooner due to the shorter combustion duration, as shown in the figure. Moreover,

(CC) 2026 Serbian Chemical Society.

the maximum *HRR* value increases with higher *CR*s as a result of the reduced ignition delay period. The maximum *HRR* values were determined to be 63.65, 67.34 and 67.49 J $^{-}$°CA for *CR*s of 15, 16, and 17, respectively. Fig. 2c depicts the variation in pressure rise rate (*PRR*) at full load for different *CR*s. As the *CR* increases, the *PRR* begins to rise earlier and reaches its highest value at a *CR* of 17, as shown in the figure. The maximum *PRR* values were determined to be 6.04, 6.15 and 7.05 bar $^{-}$°CA for *CR*s of 15, 16, and 17, respectively. These results indicate that increasing the *CR* beyond a certain level may lead to knocking, which adversely affects engine performance.

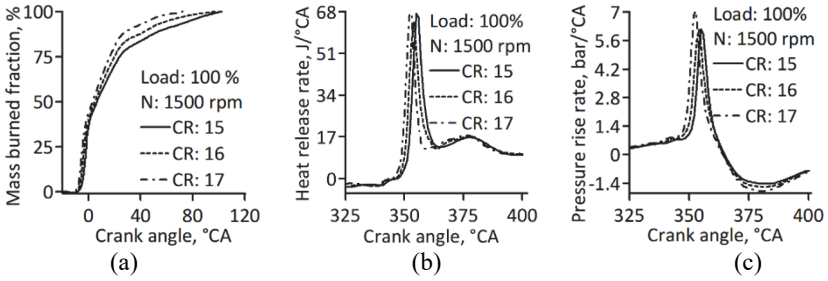

Fig. 2. Variations in: a) mass burned fraction, b) heat release rate and c) pressure rise rate.

Fig. 3a and b shows the variations in cylinder pressure and temperature with crank angle at full load for different *CR*s. Both cylinder pressure and temperature rise rapidly with the onset of combustion, and this increase occurs earlier as the *CR* rises, as illustrated in the figures. This behavior is attributed to the shortened ignition delay period at higher *CR*s, resulting in earlier combustion. Consequently, higher maximum values of cylinder pressure and temperature were achieved with increasing *CR*. Conversely, cylinder pressure and temperature began to decline earlier during the expansion process due to a shorter ignition delay and combustion duration, leading to lower values at the end of the expansion. The maximum cylinder pressures were determined to be 61.81, 65.07 and 69.31 bar, while the maximum cylinder temperatures were found to be 1319.31, 1424.63 and 1456.38 °C for *CR*s of 15, 16, and 17, respectively.

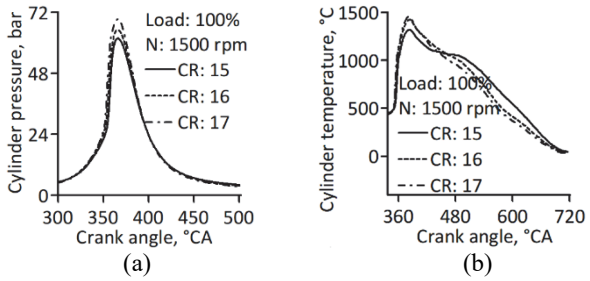

Fig. 3. Variations in: a) cylinder pressure and b) cylinder temperature.

(CC) 2026 Serbian Chemical Society.

Fig. 4a and b presents the variations in energy converted to work (E_W) and the ratio of E_W (E_W/E_f) with engine load at 1500 rpm for different *CR*s. Both E_W and its ratio increase significantly with rising engine load, which is attributed to the greater amount of fuel supplied to the cylinder at higher loads. Conversely, while the absolute E_W values did not vary considerably with *CR*, the ratio of E_W generally exhibited an increasing trend at higher *CR*s. This improvement is explained by enhanced combustion efficiency at elevated *CR*s, resulting in a larger fraction of fuel energy being converted into useful work.[23] It was determined that the E_W ratio increased by 4.7–9.9 and 4.6–17.4 % for *CR*s of 16 and 17, respectively, compared to a *CR* of 15 depending on engine load, while a reduction of 2.3 % was also observed at a *CR* of 16.

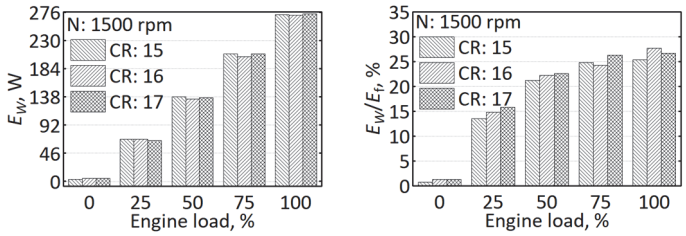

Fig. 4. Variations in: a) energy converted to work and b) ratio of energy converted to work.

Fig. 5a and b shows the variations in energy lost by heat transfer (E_{cw}) and the ratio of E_{cw} (E_{cw}/E_f) with engine load at 1500 rpm for different *CR*s. As shown in Fig. 5a, the amount of E_{cw} increases notably with rising load, which is attributed to higher combustion temperatures resulting from greater fuel supply to the cylinder. The E_{cw} ratio was lower at minimum and maximum loads (0 and 100 %), while it exhibited an increasing trend at medium loads (25–75 %). This behavior is explained by lower combustion temperatures at low loads and shorter combustion durations at high loads. Conversely, although the absolute E_{cw} values increased with *CR*, the E_{cw} ratio generally showed a stronger tendency to rise with higher *CR*s. This is attributed to increased heat loss caused by elevated combustion temperatures and longer combustion durations at higher *CR*s.[24] It was determined that the E_{cw} ratio increased by 6.4–19.5 and 5.8–24.7 % for *CR*s of 16 and 17, respectively, compared to a *CR* of 15 depending on engine load, while a reduction of 2.3 % was also observed at a *CR* of 16.

Fig. 6a and b shows the variations in energy lost through exhaust (E_{exh}) and the ratio of E_{exh} (E_{exh}/E_f) with engine load at 1500 rpm for different *CR*s. As illustrated, both the amount and ratio of E_{exh} increase notably with rising load. This is attributed to the greater fuel supply at higher loads, which results in an increase in combustion energy release, elevated combustion temperatures, and extended combustion duration.[20] Conversely, the amount and the ratio of E_{exh}

(CC) 2026 Serbian Chemical Society.

generally exhibited a slight upward trend with increasing *CR*, which is explained by higher in-cylinder pressures and temperatures at elevated *CR*s. These conditions lead to higher exhaust gas temperatures, and consequently greater energy carried away by the exhaust gases.[25] It was determined that the E_{exh} ratio increased by 4.4–17.1 and 13–21 % for *CR*s of 16 and 17 respectively, compared to a *CR* of 15 depending on engine load, while reductions of 0.6–3.6 and 0.7 % were also observed at the same *CR*s.

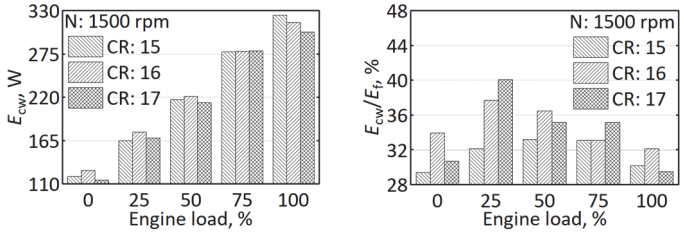

Fig. 5. Variations in: a) energy lost with heat transfer and b) ratio of energy lost by heat transfer.

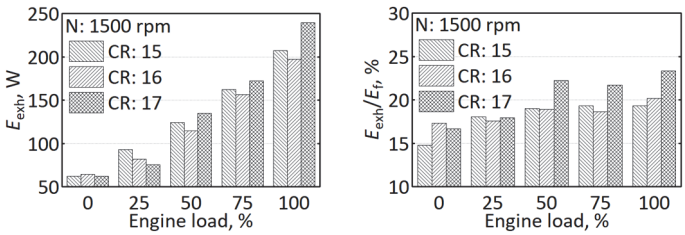

Fig. 6. Variations in: a) energy lost with exhaust and b) ratio of energy lost with exhaust.

Fig. 7a and b illustrates the variations in other energy losses (E_{other}) and the ratio of E_{other} (E_{other}/E_f) with engine load at 1500 rpm for different *CR*s. In ICEs, most other energy losses arise from combustion inefficiencies, friction losses, auxiliary power usage and fundamental thermodynamic limitations.[26] As shown in Fig. 7a, the amount of E_{other} initially decreases with rising load, then increases again, resulting in lower values at medium loads (50–75 %). This behavior is attributed to the fact that energy dissipated to auxiliary equipment remains relatively constant, even though the engine produces more work as load increases. Conversely, both the amount and ratio of E_{other} generally tend to decrease with higher *CR*s. This reduction is explained by the increase in E_W and the improvement in combustion efficiency at elevated *CR*s, which lead to lower losses.[27] It was determined that the E_{other} ratio decreased by 15.5–20.2 and 8.6–28 % for *CR*s of 16 and 17, respectively, compared to a *CR* of 15 depending on engine load, while an increase of 5.4 % was also observed at a *CR* of 16.

(CC) 2026 Serbian Chemical Society.

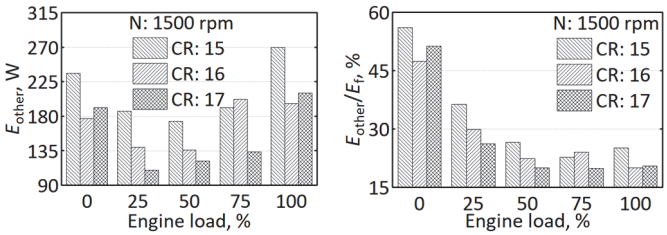

Fig. 7. Variations in: a) other energy losses and b) ratio of other energy losses.

Fig. 8a and b shows the variations in brake specific fuel consumption (*BSFC*) and energy (thermal) efficiency with engine load at 1500 rpm for different *CR*s. As shown in Fig. 8a, *BSFC* decreases significantly with rising engine load, which is attributed to the increase in work (power) produced at higher loads. Conversely, *BSFC* generally tends to decrease with increasing *CR*, due to elevated cylinder pressure and temperature that promote a more homogeneous fuel–air mixture and enhance combustion efficiency.[23] *BSFC* was reduced by 2.5–9.4 and 5–15.6 % for *CR*s of 16 and 17, respectively, compared to a *CR* of 15, depending on engine load. Furthermore, higher *CR*s were noted to improve volumetric efficiency and reduce *BSFC*, as a shortened ignition delay enhances combustion efficiency.[21] A higher *CR* compresses the air–fuel mixture further before ignition, leading to increased cylinder temperature and pressure, which results in greater energy conversion and higher power output. As shown in Fig. 8b, energy efficiency increased with both rising load and *CR*, which was attributed to improved combustion efficiency and consequently higher work output. It was observed that increasing *CR* reduces the fuel required to achieve the same power, while simultaneously improving combustion efficiency and reducing losses, thereby enhancing energy efficiency.[28] It was determined that energy efficiency increased by 4.7–9.8 and 4.9–17.4 % for *CR*s of 16 and 17, respectively, compared to a *CR* of 15, depending on engine load, while a reduction of 2.2 % was also observed at a *CR* of 16.

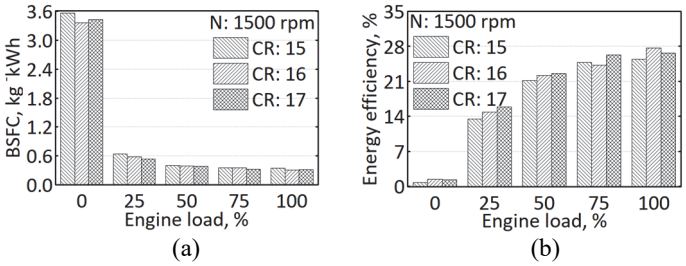

Fig. 8. Variations in: a) *BSFC* and b) energy efficiency.

Fig. 9a and b presents the variations in exergy converted to work ($E_{\chi W}$) and the ratio of $E_{\chi W}$ ($E_{\chi W}/E_{\chi f}$) with engine load at 1500 rpm for different *CR*s. As

(CC) 2026 Serbian Chemical Society.

seen in Fig. 9a, both the amount of $E_{\chi W}$ and its ratio increase significantly with rising engine load. This behavior is attributed to the greater fuel supply at higher loads, and the enhanced work output resulting from improved combustion efficiency. Conversely, although the absolute $E_{\chi W}$ values did not vary considerably with *CR*, the $E_{\chi W}$ ratio generally exhibited an increasing trend with higher *CR*s. This improvement is explained by the rise in combustion efficiency at elevated *CR*s, which enables a larger fraction of exergy input ($E_{\chi f}$) to be converted into useful work. The $E_{\chi W}$ ratio was found to increase by 9.9–22.1 and 4.9–17.4 % for *CR*s of 16 and 17, respectively, compared to a *CR* of 15, depending on engine load.

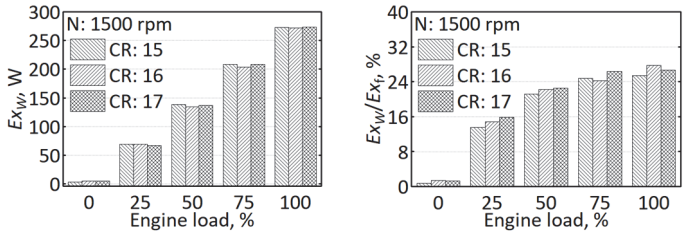

Fig. 9. Variations in: a) exergy converted to work and b) ratio of exergy converted to work.

Fig. 10a and b illustrates the variations in exergy lost through heat transfer ($E_{\chi cw}$) and the ratio of $E_{\chi cw}$ ($E_{\chi cw}/E_{\chi f}$) with engine load at 1500 rpm for different *CR*s. As shown in Fig. 10a, both the amount and the ratio of $E_{\chi cw}$ increased significantly with rising engine load. This behavior is attributed to higher combustion temperatures and changes in combustion duration as more fuel is supplied to the cylinder at increased loads. Conversely, although the amount of $E_{\chi cw}$ did not vary considerably with *CR*, the $E_{\chi cw}$ ratio generally exhibited a notable upward trend with increasing *CR*. This is explained by the rise in combustion temperature at higher *CR*s, which leads to greater heat losses.[29] The $E_{\chi cw}$ ratio was found to increase by 19.1–37.6 and 5.6–40.9 % for *CR*s of 16 and 17, respectively, compared to a *CR* of 15, depending on engine load.

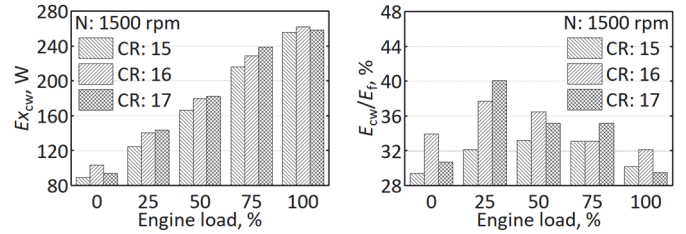

Fig. 10. Variations in: a) exergy lost by heat transfer and(b) ratio of exergy lost by heat transfer.

(CC) 2026 Serbian Chemical Society.

Fig. 11a and b illustrates the variations in exergy lost through exhaust ($E_{\chi exh}$) and the ratio of $E_{\chi exh}$ ($E_{\chi exh}/E_{\chi f}$) with engine load at 1500 rpm for different *CR*s. As shown in Fig. 11a, both the amount and the ratio of $E_{\chi exh}$ increased significantly with rising engine load. This is attributed to the greater fuel supply to the cylinder at higher loads, which results in elevated combustion temperatures and the expulsion of exhaust gases at higher pressures and temperatures. Conversely, although the amount of $E_{\chi exh}$ did not vary considerably with *CR*, the $E_{\chi exh}$ ratio generally exhibited a notable upward trend with increasing *CR*. This behavior is explained by the rise in combustion temperature at higher *CR*s, leading to exhaust gases being discharged at higher temperatures and pressures. It has been reported that improved combustion efficiency and elevated *CR*s contribute to increased combustion temperature and pressure, thereby causing higher $E_{\chi exh}$. Moreover, it has been noted that the energy carried by exhaust gases can be recovered and converted into mechanical energy through a turbocharger system, thus enhancing engine performance.[30] It was determined that the Ex_{exh} ratio increased by 7.8–17.5 and 1.8–20.9 % for *CR*s of 16 and 17, respectively, compared to a *CR* of 15, depending on engine load.

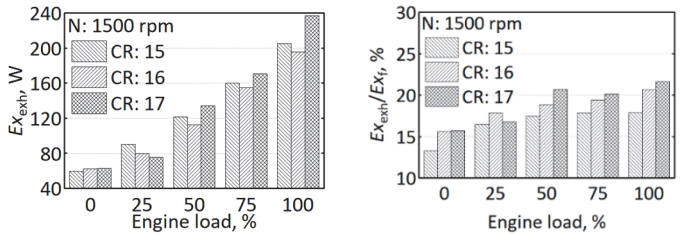

Fig. 11. Variations in: a) exergy lost with exhaust and b) ratio of exergy loss with exhaust.

Fig. 12a and b illustrates the variations in exergy destruction ($E_{\chi dest}$) and ratio of $E_{\chi dest}$ ($E_{\chi dest}/E_{\chi f}$) with engine load at 1500 rpm for different *CR*s. $E_{\chi dest}$ represents the losses arising from irreversible processes such as mixture formation, combustion, friction, and power dissipated by auxiliary equipment, and it is recognized as an important parameter for assessing the thermodynamic performance of an engine. Combustion, in particular, is a highly irreversible process; although the total energy remains constant during the conversion of fuel chemical energy to heat, exergy decreases significantly during combustion.[18] As shown in Fig. 12a, $E_{\chi dest}$ initially decreases with increasing engine load, reaches lower values at medium loads (25–75 %) and then rises again. This trend is attributed to the greater fuel consumption at higher loads, which leads to increased entropy production and consequently higher irreversibilities.[19] Moreover, longer combustion durations resulting from extended fuel injection at elevated loads cause the formation of more residual gas, thereby increasing exergy losses.[20] The $E_{\chi dest}$ ratio, however,

(CC) 2026 Serbian Chemical Society.

decreases notably with rising engine load, which is explained by higher combustion temperatures and improved combustion efficiency at increased engine loads. $E_{\chi dest}$ was found to decrease by 23.1–39.7 and 20.1–38.3 % for *CR*s of 16 and 17, respectively, compared to a *CR* of 15, depending on engine load. Conversely, both the amount and ratio of $E_{\chi dest}$ generally declined with increasing *CR*. This reduction is attributed to higher combustion temperatures and efficiency at elevated *CR*s. Enhanced thermal efficiency at higher *CR*s enables a larger portion of fuel chemical exergy to be converted into work, thereby reducing exergy losses.[31] It was found that the $E_{\chi dest}$ ratio decreased by 13.5–36.4 and 10.1–24.5 % for *CR*s of 16 and 17, respectively, compared to a *CR* of 15, depending on engine load.

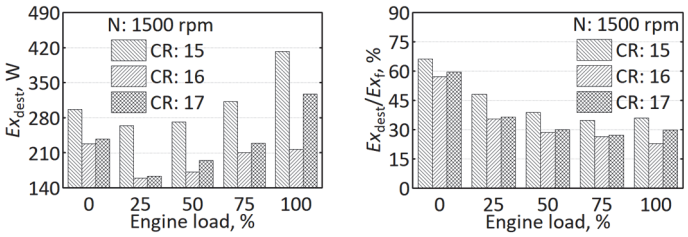

Fig. 12. Variations in: a) exergy destruction and b) ratio of exergy destruction.

Fig. 13a) and b presents the variations in $E_{\chi f}$ and exergy efficiency with engine load at 1500 rpm for different *CR*s. $E_{\chi f}$ increases with rising engine load, while it tends to decrease slightly with higher *CR*s, as shown in Fig. 13a. This behavior is attributed to the greater amount of fuel supplied to the cylinder and thus to higher fuel energy at increased loads.[32] $E_{\chi f}$ was found to decrease by 11.1–18.2 and 4.3––18.2 % for *CR*s of 16 and 17, respectively, compared to a *CR* of 15, depending on engine load. This reduction is thought to result from the lower fuel energy associated with higher *CR*s. Conversely, exergy efficiency increased with both engine load and *CR*, which is explained by improvements in combustion efficiency under these conditions. It has been reported that high combustion instability and low combustion temperature reduce exergy efficiency at low loads, whereas rising combustion temperature enhances combustion efficiency and stability, thereby improving exergy efficiency as load increases. Additionally, the higher quantity and temperature of residual exhaust gases generated at elevated loads preheat the fresh charge, increasing combustion temperature and efficiency, and contributing to higher exergy efficiency.[20] Although higher *CR*s increase combustion temperature, leading to greater heat losses and thermal irreversibilities, exergy efficiency may still improve because the gains in combustion and thermal efficiency outweigh these losses.[33] Exergy efficiency was observed to increase by 9.9–22.1 and 4.9–17.4 % for *CR*s of 16 and 17, respectively, compared to a *CR* of 15, depending on engine load. These variations highlight the dual effect of *CR*: although slight

(CC) 2026 Serbian Chemical Society.

reductions in efficiency occur at the highest *CR*, the overall trend demonstrates that increasing *CR* contributes to improved combustion efficiency and reduced irreversibilities, thereby enhancing exergy performance.

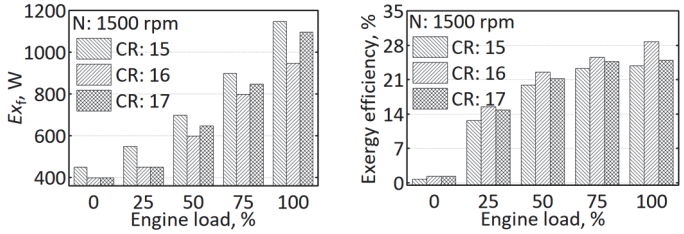

Fig. 13. Variations in: a) fuel exergy and b) exergy efficiency.

Fig. 14a and b illustrates the variations in the exergy performance coefficient (*EPC*) and sustainability index (*SI*) with engine load at 1500 rpm for different *CR*s. Both *EPC* and *SI* increased with rising engine load and *CR*, which is attributed to improved combustion stability, resulting in higher work output and exergy efficiency. It has been reported that the greater amount of fuel and air supplied to the cylinder at higher loads enhances the energy potential in the combustion chamber, thereby increasing *EPC*.[18] Conversely, an *SI* value greater than one indicates more efficient energy utilization with minimal losses in ICEs. *SI* increases with higher power output while decreasing with rising exergy destruction. Exergy efficiency also positively influences *SI*, and a higher *SI* value makes the energy source or process under investigation more attractive.[22] *EPC* was found to decrease by 45.3––110.9 and 26.7–99.9 % for *CR*s of 16 and 17, respectively, compared to a *CR* of 15, depending on engine load. Similarly, *SI* increased by 0.6–6.9 and 0.5–2.6 % for *CR*s of 16 and 17, respectively, compared to a *CR* of 15, depending on engine load. Based on these results, a *CR* of 16 appears to provide more favorable exergetic outcomes among the tested *CR*s. These findings indicate that although minor reductions occur at the highest *CR*, the overall trend demonstrates that higher *CR*s enhance *EPC* and *SI*, reflecting improved combustion stability, reduced irreversibilities, and more suitable energy utilization.

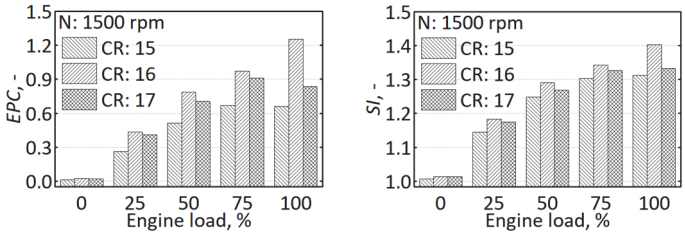

Fig. 14. Variations in: a) exergy performance coefficient and b) sustainability index.

(CC) 2026 Serbian Chemical Society.

CONCLUSION

This study provides a comprehensive thermodynamic analysis of the effects of the compression ratio (*CR*) on the combustion, performance, energy, and exergy characteristics of a diesel engine. Based on the findings, the following conclusions can be drawn.

– It was found that increasing the *CR* shortened the ignition delay, initiated combustion earlier, and completed the combustion process in a shorter duration. Consequently, higher *CR* values resulted in increased cylinder pressure and temperature, leading to improvements in efficiency and reduced fuel consumption. However, elevated pressure and temperature levels may raise production costs, as the engine requires stronger and higher–quality components during manufacturing.

– It was observed that increasing engine load and *CR* enhanced the conversion of fuel energy into work, thereby improving thermal efficiency. On the other hand, while energy losses due to heat and exhaust rose with higher engine load and *CR*, other forms of energy losses generally declined as *CR* increased.

– It was determined that increasing the engine load and *CR* enhanced the exergy converted into work, thereby improving exergy efficiency. On the other hand, while heat transfer and exergy losses through exhaust increased with higher *CR*s, exergy destruction decreased, and both the exergy performance and sustainability index showed notable improvements with rising *CR*.

CR was identified as a key parameter influencing losses, efficiency, exergy, and sustainability. Among the tested *CR*s, a *CR* of 16 was found to deliver the most favorable outcomes, particularly in terms of exergy performance. Specifically, exergy efficiency, exergy performance coefficient and sustainability index increased by 9.9–22.1, 45.3–110.9 and 0.6–6.9 %, respectively, for a *CR,* of 16 depending on engine load.

NOMENCLATURE

η_{ex}	exergy efficiency, %
BP	brake power, W
$BSFC$	brake specific fuel consumption, g / kW h
$BTE(\eta_e)$	brake thermal (energy) efficiency, %
$c_{p,cw}$	specific heat of cooling water, J / kg K
$c_{p,exh}$	specific heat of exhaust gases, J / kg K
CR	compression ratio, –
E_{cw}	energy loss with heat transfer, W
E_{exh}	energy loss with exhaust, W
E_f	fuel energy, W
E_{other}	other energy loss, W
E_W	energy converted to work, W
EPC	exergy performance coefficient, –
$E_{\chi cw}$	exergy loss with heat transfer, W
$E_{\chi dest}$	exergy destruction, W

(CC) 2026 Serbian Chemical Society.

$E_{\chi exh}$	exergy loss with exhaust, W
$E_{\chi f}$	fuel exergy, W
$E_{\chi W}$	exergy converted to work, W
FP	friction power, W
IP	indicated power, W
$ISFC$	indicated specific fuel consumption, g / kW h
$ITE(\eta_i)$	indicated thermal efficiency, %
CC	cycle coefficient, CC = 1 and CC = 2 for two and four stroke engines
LHV_f	lower heating value of fuel, J
M_{cw}	flow rate of cooling water, kg / s
m_f	flow rate of fuel, kg / s
N	engine speed, rpm
SI	sustainability index, –
T	temperature, °C or K
U	uncertainty, –
V_h	stroke volume, L or m^3
W	work, W
Z	number of cylinder, –

ИЗВОД

ДЕТАЉНА ТЕРМОДИНАМИЧКА АНАЛИЗА РАДА ДИЗЕЛ-МОТОРА ПРИ РАЗЛИЧИТИМ СТЕПЕНИМА КОМПРЕСИЈЕ

HAKAN BAYRAKTAR[1] и İSMET SEZER[2]

[1]Karadeniz Technical University, Department of Mechanical Engineering, Faculty of Engineering, Trabzon, Türkiye и [2]Gümüşhane University, Department of Mechanical Engineering, Faculty of Engineering and Natural Sciences, Gümüşhane, Türkiye

У овом раду експериментално је испитан утицај степена компресије (*CR*) на карактеристике сагоревања, као и енергетске и ексергетске карактеристике дизел-мотора. У испитивањима је коришћен четворотактни, атмосферски, водом хлађени, једноцилиндрични дизел-мотор са директним убризгавањем и могућношћу промене степена компресије. Експерименти су спроведени при константној брзини обртања од 1500 rpm, при различитим оптерећењима и степенима компресије од 15:1, 16:1 и 17:1. Софтвер у оквиру експерименталне поставке израчунава аритметичку средину резултата за десет радних циклуса како би се смањио утицај варијација између појединачних циклуса и повећала тачност резултата. На основу експериментално добијених података спроведена је детаљна термодинамичка анализа у циљу испитивања карактеристика сагоревања, као и енергетских и ексергетских карактеристика мотора при различитим степенима компресије. Резултати су показали да степен компресије има значајан утицај на наведене карактеристике. Са повећањем степена компресије повећавали су се параметри сагоревања, као што су удео сагореле масе, брзина ослобађања топлоте, притисак у цилиндру и температура гасова. Слично томе, са повећањем степена компресије уочена је и тенденција побољшања показатеља перформанси мотора, укључујући ефикасност, потрошњу горива, као и укупне енергетске и ексергетске перформансе. Од испитиваних степена компресије, степен компресије 16:1 показао је најповољније резултате са аспекта ексергетске анализе. Конкретно, при степену компресије 16:1, у зависности од оптерећења мотора, ексергетска ефикасност побољшана је за 9,9–22,1 %, коефицијент ексергетских перформанси за 45,3––110,9 %, а индекс одрживости за 0,6–6,9 %.

(Примљено 31. марта, ревидирано 25. маја, прихваћено 6. октобра 2026)

(CC) 2026 Serbian Chemical Society.

REFERENCES

1. A. B. Koc, M. Abdullah, *Fuel Process. Technol.* **109** (2013) 70 (https://doi.org/10.1016/j.fuproc.2012.09.039)
2. R. Beerge, S. Devarmani, in *Diesel Engines – Current Challenges and Future Perspectives*, IntechOpen, Rijeka, 2024 (https://doi.org/10.5772/intechopen.110936)
3. L. Wargula, A. Kadirov, D. Aimukhanov, D. Ulbrich, P. Kaczmarzyk, D. Bak, B. Wieczorek, *Sustainability* **17** (2025) 10435 (https://doi.org/10.3390/su172310435)
4. H. Liu, S. Yu, T. Wang, J. Li, Y. Wang, *J. Clean. Prod.* **451** (2024) 141996 (https://doi.org/10.1016/j.jclepro.2024.141996)
5. P. J. Megía, A. J. Vizcaíno, J. A. Calles, A. Carrero, *Energy Fuels* **35** (2021) 16403 (https://doi.org/10.1021/acs.energyfuels.1c02501)
6. M. H. Bhuiyan, Z. Siddique, *Int. J. Hydrogen Energy* **102** (2025) 1026 (https://doi.org/10.1016/j.ijhydene.2025.01.033)
7. M. E. M. Soudagara, S. Shelared, D. Marghadef, P. Belkhodeh, M. Nur-E-Alami, T. S. Kiongk, S. Ramesha, A. Rajabik, H. Venuk, T. M. Y. Khanl, M. A. Mujtabam, K. Shahapurkara, M. A. Kalamo, I. M. R. Fattah, *Energy Convers. Manage.* **307** (2024) 118337 (https://doi.org/10.1016/j.enconman.2024.118337)
8. M. A. I. Malika, M. A. Kalama, M. M. Abbas, A. S. Silitonga, A. Ikram, *Energy Convers. Manage.* **313** (2024) 118643 (https://doi.org/10.1016/j.enconman.2024.118643)
9. P. C. Miles, Ö. Andersson, *Int. J. Engine Res.* **17** (2015) 6 (https://doi.org/10.1177/1468087415604754)
10. M. K. Allawi, *Int. J. Eng. Tech. Res.* **5** (2016) 66 (https://www.erpublication.org/published_paper/IJETR042155.pdf)
11. D. Lou, Y. Liu, Y. Zhang, *Energies* **18** (2025) 1656 (https://doi.org/10.3390/en18071656)
12. M. Kaplan, *Int. J. Automot. Eng. Technol.* **8** (2019) 83 (https://doi.org/10.18245/ijaet.1495032)
13. Ö. Can, E. Öztürk, E. Arcaklioğlu, *Int. J. Automot. Sci. Technol.* **5** (2021) 43 (https://doi.org/10.30939/ijastech..805531)
14. T. Grönstedt, M. Irannezhad, X. Lei, O. Thulin, A. Lundbladh, *J. Eng. Gas Turbines Power* **136** (2014) 31202 (https://doi.org/10.1115/1.4025727)
15. M. Özkan, *Entropy* **17** (2015) 244 (https://doi.org/10.3390/e17010244)
16. J. P. G. Montoya, *Appl. Therm. Eng.* **280** (2025) 128376 (https://doi.org/10.1016/j.applthermaleng.2025.128376)
17. https://www.apexinnovations.co.in/pdf/PSP240.pdf (03.04.2026)
18. K. Gupta, N. Singh, P. Goswami, A. Priyam, *Int. J. Hydrogen Energy* **163** (2025) 150712 (https://doi.org/10.1016/j.ijhydene.2025.150712)
19. R. B. Mshelia, R. Yusuf, S. Sudi, *Konya J. Eng. Sci.* **10** (2022) 18 (https://doi.org/10.36306/konjes.984008)
20. D. Erol, E. Gülcan, *Int. J. Automot. Eng. Technol.* **14** (2025) 154 (https://doi.org/10.18245/ijaet.1705733)
21. C. Tiwari, T. N. Verma, G. Dwivedi, P. Verma, *Appl. Sci.* **13** (2023) 1857 (https://doi.org/10.3390/app13031857)
22. M. Ünaldi, A. Uyaroglu, H. E. Gülcan, M. Ciniviz F. Aydin, *Int. J. Hydrogen Energy* **158** (2025) 150542 (https://doi.org/10.1016/j.ijhydene.2025.150542)
23. M. K. Rath, S. K. Acharya, P. P. Patnnaik, S. Roy, *Int. J. Eng.* **27** (2014) 1259 (https://www.ije.ir/article_72362_5cf5ccfabacae0fe6ee918ef6961bc99.pdf)

(CC) 2026 Serbian Chemical Society.

24. V. Gnanamoorthi, G. Devaradjane, *J. Energy Inst.* **88** (2015) 19 (https://doi.org/10.1016/j.joei.2014.06.001)
25. S. Verma, L. M. Das, S. C. Kaushik, *Energy Convers. Manage.* **138** (2017) 346 (https://doi.org/10.1016/j.enconman.2017.01.066)
26. V. Gajjar, V. Patel, *Int. J. Eng. Sci. Invention* **13** (2024) 38 (https://www.ijesi.org/papers/Vol(13)i6/D13063846.pdf)
27. P. Bridjesh, G. Arunkumar, *Int. J. Chem. Sci.* **13** (2015) 997
28. S. S. Bhatti, S. Verma, S. K. Tyagi, *Therm. Sci. Eng. Prog.* **9** (2019) 332 (https://doi.org/10.1016/j.tsep.2018.12.006)
29. H. Yaman, *Process. Saf. Environ. Prot.* **158** (2022) 607 (https://doi.org/10.1016/j.psep.2021.12.014)
30. S. G. Chaudhari, M. A. Modi, T. M. Patel, G. P. Rathod, *IOSR J. Eng.* **6** (2016) 13 (https://iosrjen.org/Papers/vol6_issue4%20(part-3)/D06431319.pdf)
31. M. K. Yesilyurt, *Fuel* **278** (2020) 118319 (https://doi.org/10.1016/j.fuel.2020.118319)
32. B. Wang, M. Pamminger, T. Wallner, *Appl. Energy* **254** (2019) 113645 (https://doi.org/10.1016/j.apenergy.2019.113645)
33. Z. M. Yao, Z. Q. Qian, R. Li, E. Hu, *Energy* **176** (2019) 991 (https://doi.org/10.1016/j.energy.2019.04.027).

(CC) 2026 Serbian Chemical Society.